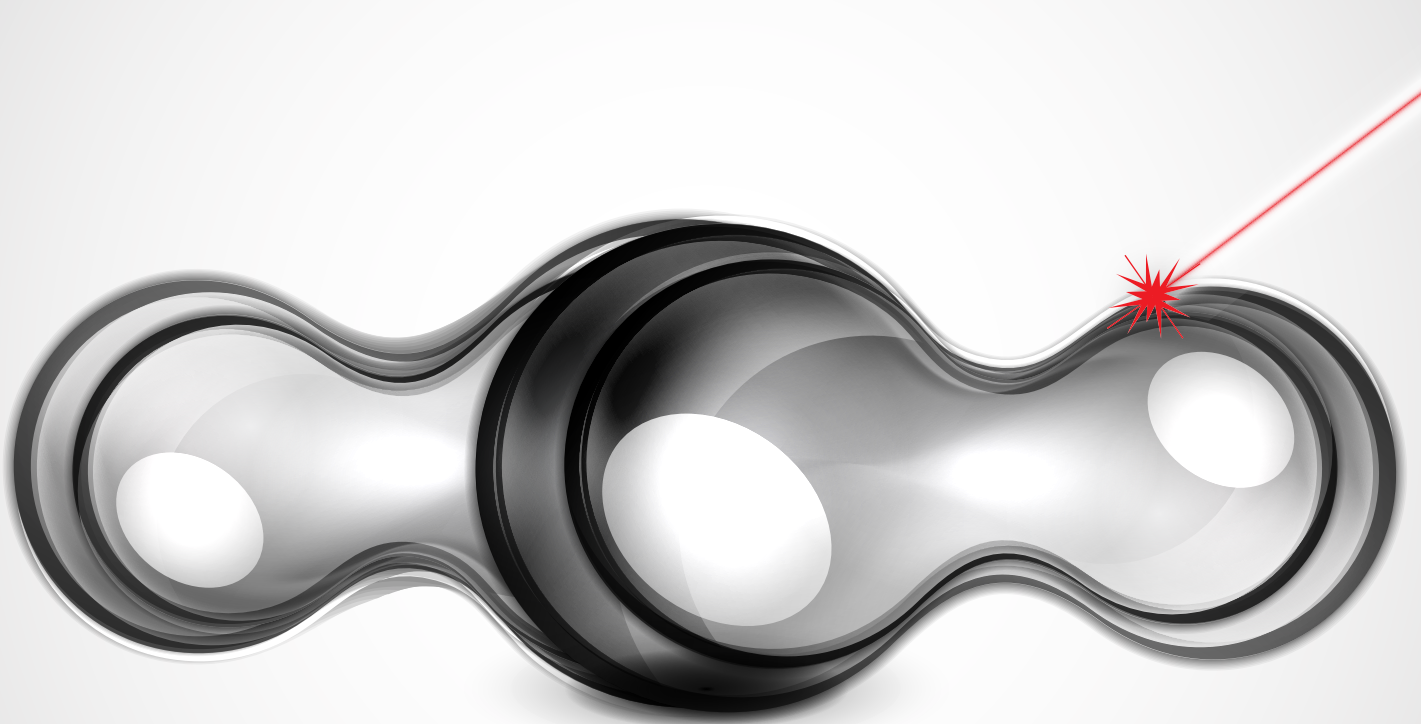




Consortium for Innovation in
Manufacturing & Materials



Proceedings
RII CIMM Symposium
June 3, 2019 • Baton Rouge, LA



Sponsored by the National Science Foundation, Louisiana Board of Regents and Louisiana EPSCoR.

Investigation of Mechanical, and Phase Properties of Refractory High Entropy Alloy MoNbTaTiW

Uttam Bhandari¹, Congyan Zhang¹, Sai Uppu¹, Xuhang Gu¹, Gregory Richard¹, Latorious Spurlock¹, Ebrahim Khosravi¹, Patrick Mensah², Dwayne Jerro², Samuel Ibekwe², Guoqiang Li³, Shengmin Guo³, and Shizhong Yang¹

¹Department of Computer Science, Southern University and A & M College, Baton Rouge, Louisiana, 70813

²Department of Mechanical Engineering, Southern University and A&M College, Baton Rouge, LA 70813

³Department of Mechanical & Industrial Engineering, Louisiana State University, Baton Rouge, LA 70803

Abstract: The refractory high entropy alloys are emerging as a new applicable material for high thermal stability. The Density functional Theory (DFT) was employed to study the mechanical properties of MoNbTaTiW. The calculated Shear modulus, Young's modulus, and Poisson's ratio are in excellent agreements with available experimental values. The calculated phase diagram of MoNbTaTiW using TCHEA1 data base shows an existence of a stable body centered cubic (BCC) phase at high temperature, which agrees with experimental results. When the composition of Ti is lowered in MoTaTiTaW alloy, increasing trend for BCC phase than HCP is observed. These findings may provide a base for a new research and application for MoNbTaTiW.

Keywords: High Entropy Alloy, MoNbTaTiW, Phase diagram, DFT.

1. Introduction

High entropy alloys (HEAs) are formed by mixing five or more elements at any combinations. These mixing changes the structure of a whole system and produces a single solid phase structure with different properties. The HEAs are often described by the four core effects, [1,2] high entropy effect, sluggish diffusion, cock-tail effect and lattice distortion. These core effects play important role in determining the different physical and mechanical properties [3]. Most HEAs are strong, superconductive and resistant to crack, fatigue, corrosion and irradiation [4].

The refractory HEAs (RHEAs) is one group of HEAs which introduces the refractory elements (for example, Mo, Nb, Ta, Ti, V, W and Hf) in HEAs. The refractory elements in HEAs may lead to a better high-temperature performance, which makes RHEAs highly applicable for aerospace industry, cryogenics, hard coating industries and high temperature refractory applications [5]. The MoNbTaTiW was developed from the previous RHEA MoNbTaW which have excellent thermal stability but very brittle at room temperature. Han et al. [6] decreased the brittleness of MoNbTaW by adding Ti. Addition of Ti to MoNbTaW increased the strength from 996 MPa to 1455 MPa. More insight on mechanical and phase properties MoNbTaTiW is necessary for applications.

2. Computational method

The Vienna Ab Initio Simulation Packages (VASP) [7] was employed to optimize the structure of MoNbTaTiW based on Density Functional Theory (DFT) [8-10]. The atomic structure of MoNbTaTiW with BCC structure was

created in Material Studio [11, 12] with total 100 numbers of atoms. The calculations were proceeded by using the projector augmented wave (PAW) potentials [13]. The generalized gradient approximation (GGA) of Perdew-Burke-Ernzerhof (PBE) [14] was applied in calculation as an exchange-correlation function. The K points sampling was done to integrate the brillouin-zone. We used the atomistic simulation tool MedeA [15] and the molecular dynamics simulation package LAMMPS [16] to calculate mechanical properties of MoNbTaTiW. The ThermoCalc-2019 software [17] was used to calculate the phase diagram, Scheil solidification simulation and total latent heat of MoNbTaTiW using the TCHEA1 [18] data base calculations. MoNbTaTiW was composed of 20% of each Mo, Nb, Ta, Ti, and W. The single point calculation was performed in order to get the detailed information about composition of elements in structure formation.

3. Results and discussions.

The calculated bulk modulus, shear modulus, Young’s modulus, Posion’s ratio, and Pugh ratio are tabulated in Table I, the experimental results performed by Han et al. [19] are also listed in the table. The excellent agreement between our results with experiments implied the accuracy of the theoretical calculation. Moreover, the high bulk module indicates high strength of MoNbTaTiW, and high pugh’s ratio indicates high ductileness of MoNbTaTiW. The BCC structure of it shown in Fig. 1. The phases diagram of MoNbTaTiW is shown in Fig. 2. The single-phase BCC is seen at high temperatures which is highly stable from 700 °C to 2400 °C. No phase change occurs within this temperature range. When the temperature is above 2700 °C, MoNbTaTiW is 100% liquid. The HCP and BCC phase is seen at low temperature. Our results are in good agreement with experiment results from Han et al. [6], which announced that the stable BCC phase in MoNbTaTiW between 1000 °C to 2500 °C, and the HCP phase exists when temperature is below 640 °C. From the single point calculation, it is found the HCP phase of MoNbTaTiW mostly consists of Ti element at low temperature and negligible contribution from other elements. As per Table. II, by lowering the Ti composition, it lowers HCP structure as well as total Gibbs free energy, the lowering of Gibbs free energy indicates the increasing stability of the system [20].

Table I. Mechanical properties of MoNbTaTiW

MoNbTaTiW	Bulk module (GPa)	Shear module (GPa)	Young’s module (GPa)	Poisson ratio (a.u)	Pugh’s ratio (a.u)
Our Calculation	246.691	54.72	152.86	0.3967	4.5212
Experimental value [19]	139	59	156	0.31	---

Table II. Phase study table of MoNbTaTiW with concentration of element (in mol. %) during formation and results from single point calculation. Contribution of Ti element in HCP formation at low temperature.

Mo (%)	Nb (%)	Ta (%)	Ti (%)	W (%)	Phase	Ti composition at low T	total Gibbs energy
20	20	20	20	20	80.0017% BCC_B2 19.983% HCP_A3	1.00	-19565.97736 [J]
21.25	21.25	21.25	15	21.25	85018% BCC_B2 14.982% HCP_A3	1.00	-20212.84182 [J]
22.5	22.5	22.5	10	22.5	90.002% BCC_B2 0.0998% HCP_A3	1.00	-20859.70627 [J]
23.75	23.75	23.75	23.75	23.75	0.95021% BCC_B2 0.04979% HCP_A3	1.00	-21506.57073 [J]

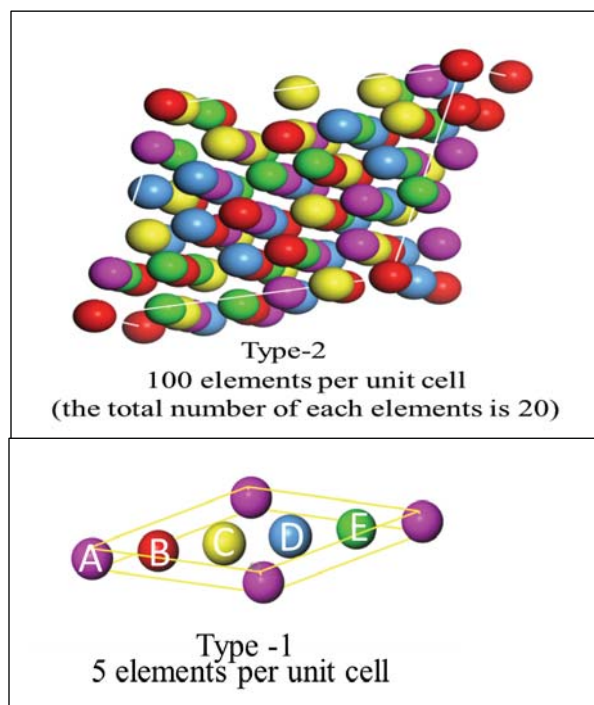


Fig. 1. Bcc structure of MoNbTaTiW

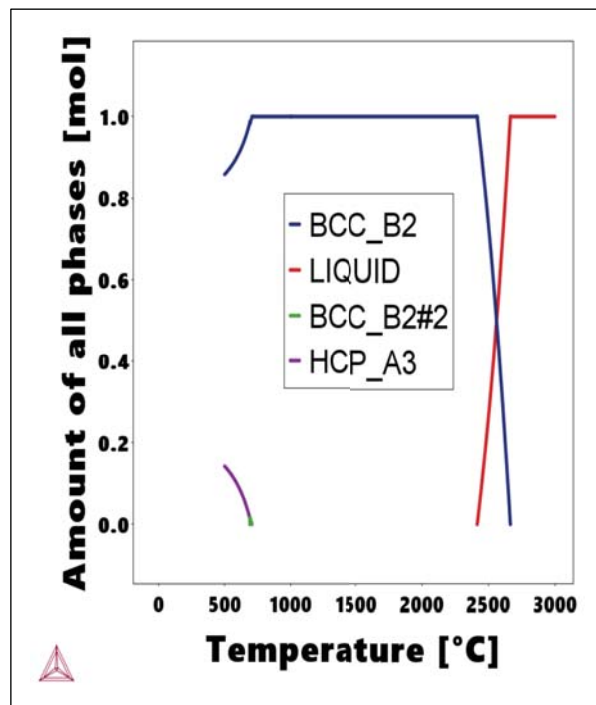


Fig. 2. Calculated, phase diagram of MoNbTaTiW.

4. Conclusion

In this report, the calculated mechanical properties of MoNbTaTiW revealed their high strength and high ductileness properties. The MoNbTaTiW only showed BCC crystal at high temperature in the range of 700°C ~ 2400 °C, the single point calculation emphasized the contribution of Ti element to the HCP phase at low temperature.

5. Acknowledgments

The current work is partially supported by the NSF EPSCoR CIMM project under award #OIA-1541079 and DoD (W911NF1910005). The Advanced Light Source is supported by the Director, Office of Science, Office of Basic Energy Sciences, of the U.S. Department of Energy (DE-AC02-05CH11231). The computation is supported by LONI computer time allocation.

6. References

- [1]. B. Cantor, I.T.H. Chang, P. Knight, A.J.B. Vincent, Mater. Sci. Eng. A 375e377 213e218 (2004).
- [2]. J.W. Yeh, S.K. Chen, S.J. Lin, J.Y. Gan, T.S. Chin, T.T. Shun, C.H. Tsau, S.Y. Chang, Adv. Eng. Mater 6 299e303 (2004)
- [3]. H.W. Yao, J.W. Qiao, J.A. Hawk, H.F. Zhou, M.W. Chen, M.C. Gao, Journal of Alloys and Compounds 696, 1139e1150 (2017)
- [4]. C. Jung, K. Kang, A. Marshal, K. G. Pradeep, J. -B. Seol, H. M. Lee, P. -P. Choi, Acta Materialia, 31-39 (2019)
- [5]. Y.J. Zhao, J.W. Qiao, S.G. Ma, M.C. Gao, H.J. Yang, M.W. Chen, Y. Zhang, materials&design 96, 10-15 (2016)
- [6]. Z.D. Han, H.W. Luan, X. Liu, N. Chen, X.Y. Li, Y. Shao, K.F. Yao. Materials Science &engineering A 712 (2018) 380-385
- [7]. G. Kresse and J. Furthmüller, Phys. Rev. B, 1996, 54, 11169-11186.
- [8]. P. Hohenberg and W. Kohn, Phys. Rev., 1964, 136, B864-B871.
- [9]. W. Kohn and L. J. Sham, Phys. Rev., 1965, 140, A1133-A1138.
- [10]. U.Bhandari, C.O. Bamba, Y. Malozovsky, L.S. Franklin, and D.Bagayoko, Journal of Modern Physics, 9, 1773-1784 (2018).
- [11]. B. Delly, J. chem phys. 92, 508 1990
- [12]. B. Delly, j. chem. Phys. 113, 7756, 2000
- [13]. P. E. Blöchl, Phys. Rev. B, 50, 17953-17979 (1994).
- [14]. P.E. Blöchl, Phys. Rev. B 50, 17953-17979 (1994)
- [15]. M. Calzarossa L. Massari, A. Merio ; M. Pantano ; D. Tessera, IEEE Systems & Applications, 72-80 (1995)
- [16]. W. M. Brown, A. Kohlmeyer, S. J. Plimpton, A. N. Tharrington, Comp Phys Comm, 183, 449-459 (2012)
- [17]. J. O. Andersson, T. Helander, L. Höglund, P.F. Shi, and B. Sundman, *Calphad*, 26, 273-312 (2002)
- [18]. H. Mao, H.-L. Chen, Q. Chen, J. Phase Equilibria Diffus. 38, 353-368 (2017).
- [19]. Z.D. Han, N. Chen, S.F. Zhao, L.W. Fan, G.N. Yang, Y. Shao, and K.F. Yao, Intermetallics 84, 153 (2017).
- [20]. F. Zhang, C. Zhang, S.L. Chen, J. Zhu, W.S. Cao, and U.R. Kattner, Computer Coupling of Phase Diagram and Thermochemistry 45, 1-10, (2014)